

# Study of fluidized bed regimes using Computational Particle Fluid Dynamics

Rajan Jaiswal Cornelius E. Agu Rajan K. Thapa Britt M. E. Moldestad

Department of Process Energy and Environmental Technology  
University College of Southeast Norway, Norway

[rajanjaiswal357@gmail.com](mailto:rajanjaiswal357@gmail.com) { [cornelius.e.agu](mailto:cornelius.e.agu), [rajan.k.thapa](mailto:rajan.k.thapa), [britt.moldestad](mailto:britt.moldestad@usn.no) }@usn.no

## Abstract

The fluidization technology has a wide range of applications. In chemical synthesis, fluidized bed is used to enhance heat and mass transfer between the reacting species. More application of this technology can also be seen in pneumatic transport and circulation of solid particles. The different applications require different flow regimes. This study investigates the influence of initial bed height on the fluidized bed regime transition using the Computational Particle Fluid Dynamics (CPFD) software, Barracuda VR. The simulations are performed for a specific powder with a narrow particle size distribution. The results from the simulations are compared with the experimental data and correlations in the literature. The minimum fluidization velocity drop to a stable value and the bubbling velocity remains constant with an increase in the bed height. The gas velocity at onset of slugging decreases while that of turbulent increases to a stable value as the bed height increases.

Keywords: *Fluidized bed, transition to bubbling regime, pressure drop, bed height, minimum fluidization velocity, CPFD*

## 1 Introduction

### 1.1 Background

Fluidization technology has wide range of applications in many processes like chemical synthesis, pneumatic transportation, chemical regeneration, powder mixtures and even in the hospitals (Hargest and Artz 1969) for example, treatment of Ulcer patient. Each application requires different regimes. The types of flow regime that can be established in a fluidized bed depend on the parameters such as superficial gas velocity, particle properties, and bed dimension. The properties of fluidized bed based on these parameters have been widely studied by many researchers (Felipe and Rocha 2007; Escudero and Heindel 2011; Sarker, Rahman et al. 2012). However, the dynamic behavior of the different fluidization regimes still needs to be investigated.

Fluidization is the process where a bed of solid particles is transferred from a static solid-like state to a

dynamic fluid-like state. Fluidized beds can extend from loose bed to pneumatic conveying depending on the inlet superficial gas velocity. The superficial gas velocity at which the frictional force between the fluid and particles are counterbalanced by the weight of the bed is said to be the minimum fluidization velocity ( $u_{mf}$ ). The pressure drop due to weight of the bed at this point is the maximum pressure drop (Kunii and Levenspiel 2013). With the increase in gas velocity, bubbles start to form and rise in the bed depending on the properties of particle. For a bed with smaller particles, the bed expands significantly before formation of bubbles occurs (Abrahamsen and Geldart 1980) while for a bed with larger particle diameter (Geldart B particle), the bubbles start to form as soon as the bed is fluidized. The onset of the bubbling regime occurs at the superficial gas velocity when the bubbles first appear in the bed and the corresponding velocity is called the minimum bubbling velocity ( $u_{mb}$ ) (Dennis 2013). With further increase in the gas velocity, the bubble rise velocity and bubble size increase (Bauer, Werther et al. 1981). When the bubble diameter is  $\sim(0.3 - 0.6) D$ , the bed slugs. Where,  $D$  is the column diameter. Different types of slug can be observed, and these include axisymmetric, squared-nose and wall slug. The type of slug flow in a fluidized bed depends on particle type, particle size, bed diameter and the wall of the column (Dennis 2013; Yates 2013). Bubble and slug flow largely influence the gas and solid interaction in the fluidized bed, thus identifying onset of bubbling and slugging regime and their transition zone is crucial for the design of a fluidized bed reactor. The slug flow shifts into turbulent with further increase in gas velocity followed by random fluctuation of pressure drop. The turbulent regime is marked with the absence of bubbles and slugs in the bed and is followed by violent movement of elongated and distorted voids and particles. Increasing the superficial gas velocity beyond the bubbling velocity for fluidized beds of small particles, the fluctuation in pressure drop reaches a peak. The gas velocity at the peak pressure drop fluctuation is regarded as the critical velocity ( $u_c$ ) as shown in Figure 1. Beyond  $u_c$ , the fluctuation decreases until it reaches a steady value. The minimum gas velocity at which the pressure fluctuation is relatively constant is denoted by

$u_k$  (Yerushalmi and Cankurt 1979). Between the gas velocities  $u_c$  and  $u_k$ , the fluidized bed is in turbulent flow regime.

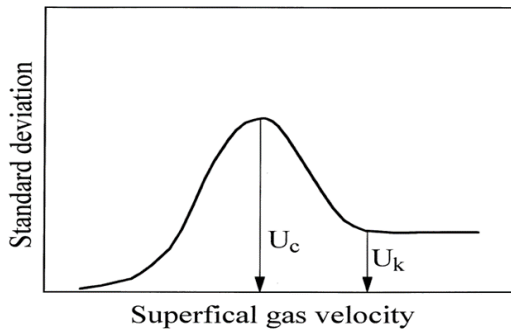


**Figure 1.** Amplitude of pressure Fluctuation with increase in gas velocity.

In the case of coarse particles, for instant Geldart D particles, large exploding bubbles are observed before it reaches the turbulent regime. Once the turbulent regime is established, severe gas channeling and then large-scale uniform circulation of bed material termed churning fluidization follow. Different regimes in a fluidized bed can be identified following different approaches. However, statistical method i.e. standard deviation of pressure fluctuation is the simplest and most economical (Vial, Camarasa et al. 2000).

In this work, minimum fluidization, bubbling, slug and turbulent regimes are obtained using a Computational Particle Fluid Dynamic (CPFD) model. The CPFD simulation is based on the Barracuda code, and the model is further validated using experimental results. The onset and transition of each regime are obtained from variation of pressure drop fluctuation (standard deviation) with gas velocity at five different aspect ratios. The standard deviation ( $\sigma$ ) of pressure fluctuation is calculated from

$$\sigma = \sqrt{\frac{\sum_{i=1}^N (P_i - \bar{P})^2}{N-1}} \quad (1)$$

where,  $\bar{P}$  is the mean pressure and  $N$  is the number of data set. Similar to Figure 1, the change in standard deviation of pressure fluctuation is used to identify the onset or transition of one regime to another. The point where there is a change in the slope of the standard deviation curve marks the onset of one regime to another. This method has been used by different researches to identify the minimum fluidization velocity and quality of fluidization (PunČochÁŘ et al. 1985; Chong et al., 1987; Hong et al., 1990; Felipe and Rocha, 2007). Moreover, different fluidized bed regimes obtained using the standard deviation method have been compared with other techniques (Gourichl et al., 2006; Tchowa Medjiade et al., 2017). (Yerushalmi and

Cankurt, 1979) identified turbulent flow regimes with two transition velocities as shown in Figure 1. (Bi et al., 2000) identified transition of turbulent regime using the standard deviation method and then reported that the value of  $u_c$  for the onset of turbulent regime is higher for methods based on differential pressure measurement than those based on absolute pressure.

## 2 Experimental and Simulation Setup

### 2.1 Experimental Setup

The experimental set up used in this work consists of a 3D transparent cold bed column of height ( $h$ ) 1.5 m and diameter ( $D$ ) 0.084 m. A set of pressure transducers are connected to the pressure tapping points installed along the wall of the column. The distance between two consecutive pressure points along the column height is 10 cm. Compressed air at an ambient condition is supplied through an air supply hose fitted at the plenum below a porous plate distributor. The flow of air into the column is controlled by the air control valves attached to the rig. LabVIEW, a data acquisition software, is used to record the pressure drop along the column height. Figure 2 shows the experimental set up used in this work.

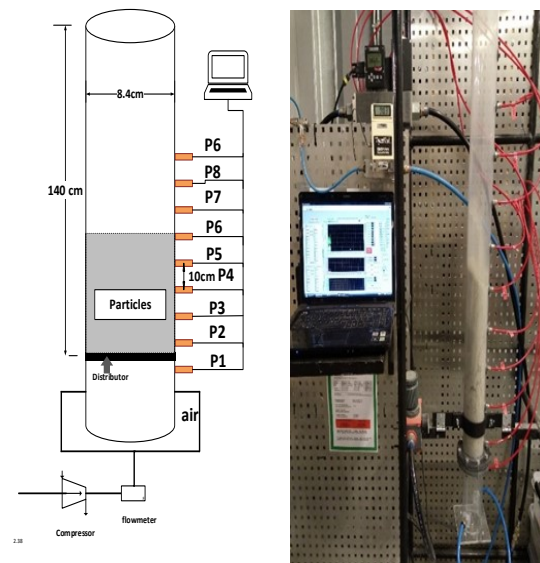


**Figure 2.** Experimental set-up for a cold fluidized bed.

### 2.2 Simulation Setup

Simulation tool such as the CPFD Barracuda code is not only used to optimize the cost, energy and time but can also be used to solve the major experimental challenges. Due to the limited height of the experimental set up, identifying the turbulent regime in the experiment is impossible. However, with the use of the Barracuda code in this study, all the regimes for sand particle based on five different aspect ratios ( $h_0/D$ ): 0.7, 1, 1.5, 2, 2.5 are obtained.  $h_0$  is the static bed height.

A cylindrical CAD geometry with the column height 300 cm and diameter 8.4 cm is imported into the

Barracuda VR software. Uniform grid of total 10000 cells is generated around the geometry for the simulations. The bottom of the column is set as inlet flow boundary condition while the top of the column is considered as the pressure boundary condition (as in the experimental set up). Thus, gas flow is uniform throughout the column with no boundary layer around the walls. The cells with volume fraction less than 0.04 and aspect ratio greater than 15:1 are removed since default grids are generated using default grid settings. The, pressure boundary conditions, CAD geometry, grid, flow, and transient data locations are shown in Figure 3.

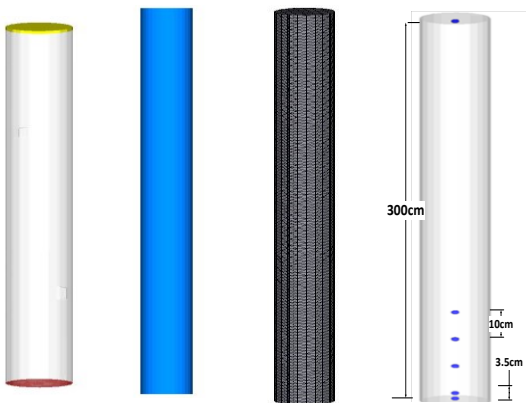


**Figure 3.** Simulation geometry showing from the left side the pressure boundary condition, the CAD geometry, the grid arrangement and the transient data locations.

The particle size distribution and close pack volume fraction used for the simulations are the same as in the experiments. The maximum momentum from redirection of particles collision were assumed to be 40% with the normal-to-wall and tangential-to-wall momentum retention as 0.3 and 0.99, respectively. The particle properties and operating conditions used in the simulations are summarized in Tables 2 and 3, respectively. The monitoring points were used at the middle of the column that resembles the pressure transducers height in the experiment.

Table 1. Operating conditions

Fluidizing gas	Air
Fluid temperature	Ambient (300K)
Superficial gas velocity	0.016 to 2 m/s
Static bed height	(0.7, 1, 1.5, 2, 2.5)·D
Outlet pressure	101325 Pa

Table 2. Particle and bed properties.

Sand Particles			
Particle mean diameter	234.74 $\mu\text{m}$		
Density	2650 $\text{kg}/\text{m}^3$		
Bulk density	1388 $\text{kg}/\text{m}^3$		
Solid void fraction	0.52		
Particle size distribution			
Sieve range ( $\mu\text{m}$ )	Mean diameter ( $\mu\text{m}$ )	Weight fraction	Cumulative frequency (%)
100-150	125	0.028	2.84
150-200	175	0.116	14.42
200-250	225	0.321	46.48
250-300	275	0.535	100

### 3 Results

#### 3.1 Validation of CPFD model

To establish the valid model for further simulations, the simulations and experiments were carried out with sand particles of size 235  $\mu\text{m}$  and aspect ratio ( $h_0/D$ ) 2.5, and the minimum fluidization velocity obtained by plotting pressure drop versus superficial gas velocity are compared. Figure 4 shows the simulated pressure drop based on two different drag models: Wen and Yu and a combination of Ergun and Wen & Yu models. As compared with experimental data, the figure shows that the results from both models agree well with the experimental data when the bed is in fluidized state.

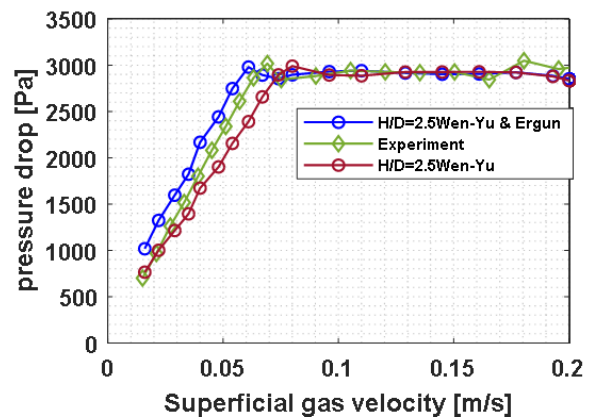


**Figure 4.** Pressure drop with superficial gas velocity for different bed aspect ratios.

However, while the Wen and Yu model over-predicts the gas velocity at the onset of fluidization, the combined Ergun and Wen & Yu model under-predicts the data but with a slightly lower deviation. The deviation using the Ergun and Wen & Yu and drag model is approximately 9%. Thus, the Ergun and Wen & Yu drag model is considered as acceptable to be used in the rest of the work.

The figure clearly shows that with increasing superficial gas velocity the pressure drop increases and reach a peak value identified as the maximum pressure

drop. At the maximum pressure drop, the minimum fluidization velocity  $U_{mf}$  is noted. Above  $U_{mf}$ , the bed pressure drop remains almost constant.

### 3.2 Onset of different fluidization regimes

For the bed aspect ratio 0.7, Figure 5 shows the variation of the simulated pressure fluctuation (standard deviation) at the middle of the bed. The pressure fluctuation remains almost zero until a superficial gas velocity denoted by  $U_{mb}$ , which describes the onset of bubbling in the bed. Beyond the value of  $U_{mb}$ , the fluctuation increases rapidly due to coalescence of bubbles. As gas velocity is increased, the bubble size increases. When the bubble grows to become a slug, the rate of change of the pressure fluctuation with the gas velocity decreases. The gas velocity at which the bed begins to slug is denoted by  $U_{ms}$ . With further increase in the gas velocity up to  $U_c$ , the gas slug explodes, leading to rapid fluctuation of the bed. For the gas velocity above  $U_c$ , the bed fluctuation decreases. The gas velocity  $U_c$  presents the onset of the turbulent flow regime. The decrease in the bed fluctuation with increasing gas velocity in the turbulent flow regime is associated with expansion of the bed where the particles are relatively far from each other. The particle separation increases with increasing gas velocity in this regime and may reach a constant value at very high velocity. For each of the regimes identified in Figure 5, the fluctuation of solids fraction in the bed is shown in Figure 6. Within the time interval 80 - 90 s for gas velocity of 0.064 m/s, it can be seen that the particle

solid volume fraction decreased from 0.52 to a value of about 0.5, marking the point of minimum fluidization condition.

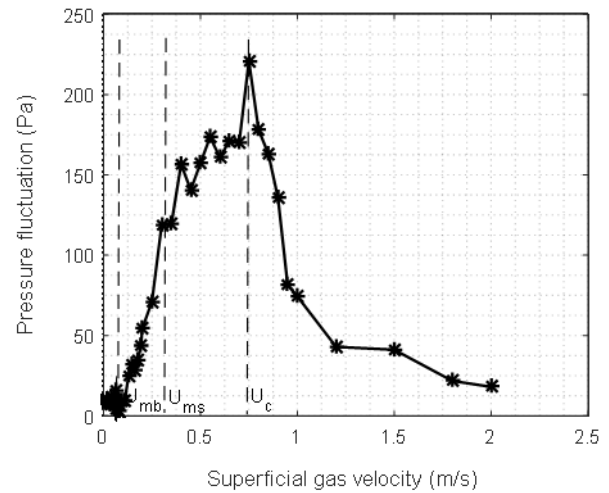


**Figure 5.** Pressure drop fluctuation showing the onset of different fluidized bed regimes.

The solid fraction remained constant up to 100 s and started to drop from 0.5 to 0.35 in the period of 100 - 110 s and flowrate 0.07, marking the onset of bubbling regime. Similarly, the onset of slugging regime is identified at the flowrate of 0.25 m/s and time period 190 - 200 s. The onset of turbulent regime can be confirmed at the flow rate of 0.75 m/s and at time 290 - 300 s. At this gas velocity, the fluctuation in solids fraction is vigorous, corresponding to the peak value of the pressure fluctuation in Figure 5.

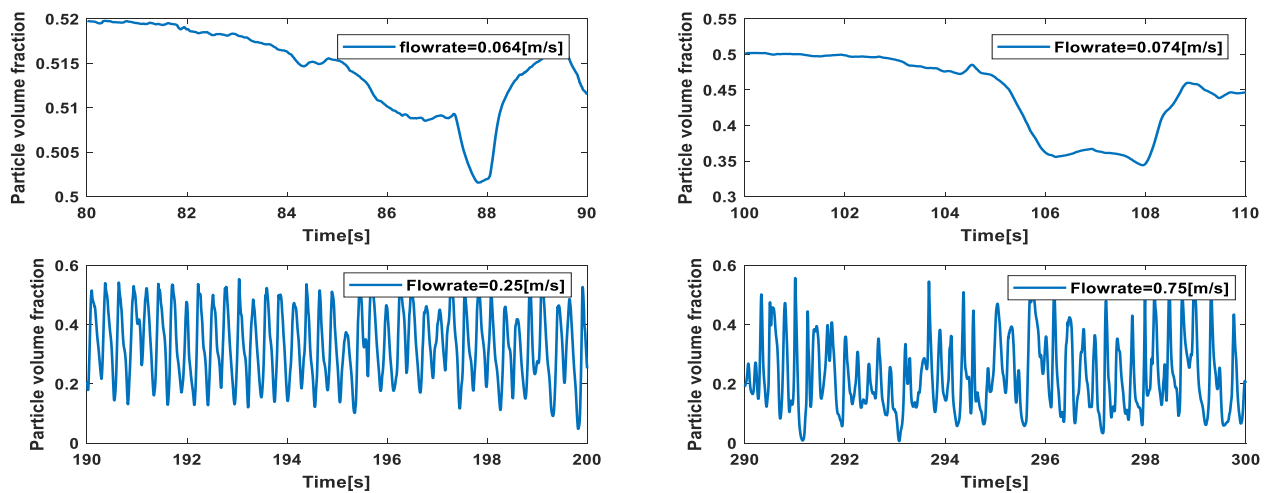


**Figure 6.** Change in particle volume fraction at the onset of different fluidized bed regimes (a) minimum fluidization velocity (B) minimum bubbling regime (C) minimum slugging regime (D) minimum turbulent flow regime.

### 3.3 Minimum fluidization and bubble velocity

The minimum fluidization velocities simulated at different bed aspect ratios are shown in Figure 7. The value of  $U_{mf}$  drops slightly from a value at a lower aspect ratio aspect ratio  $h_0/D < 1.5$  to a value at a higher aspect ratio. A similar trend is also observed from the experimental results, but in a reverse order. Figure 7 also shows that the gas velocity at onset of bubbling is independent of the initial bed height. This indicates that when the bed is shallow  $h_0/D < 2$ , the bed begins to bubble as soon as it is fluidized. However, in a deeper bed, the result shows that the bed expands before bubbles begin to flow.

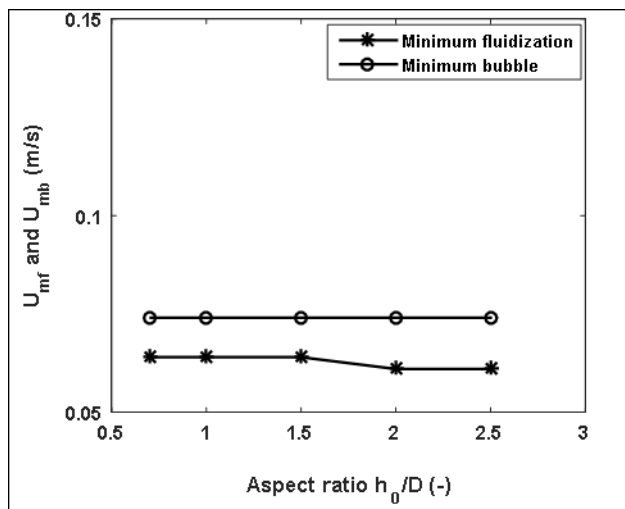


**Figure 7.** Variation of minimum fluidization velocity and bubbling velocity with different bed aspect ratios.

### 3.4 Minimum slugging velocity

The gas velocity at the onset of slugging regime is simulated for different aspect ratios. Figure 8 compares the minimum slugging velocity obtained from the CPF D simulations with the experimental data. The prediction of  $U_{ms}$  using different models are also shown. As can be seen, there is a good agreement between the simulated result and the experimental data for all aspect ratios. Similar to the experimental data, the predicted results show that the gas velocity at onset of slugging decreases with an increase in the aspect ratio.

The Baeyens and Geldart (1974) model under predicts the experimental data for all aspect ratios. The experimental data agree well with the Agu et al. (2018) model for  $h_0/D < 1.5$ . Particles with sphericity of 0.85 are assumed in the Agu et al. model.

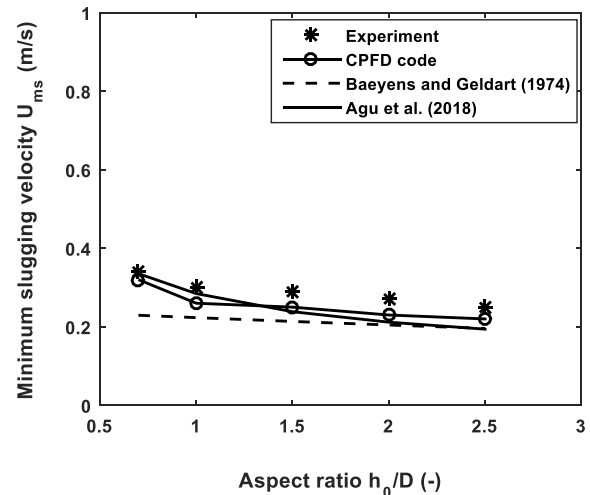


**Figure 8:** Variation of minimum slugging with different bed aspect ratios compared with the experimental data and different correlations

### 3.5 Onset of turbulent flow regime

Figure 9 shows a comparison of the simulated value of  $U_c$  with the result predicted based on Bi and Grace (1995). The simulation shows that at onset of turbulent regime, the gas velocity increases with an increase in the bed aspect ratio in the range  $0 < h_0/D < 1.5$ . In the deeper bed,  $U_c$  is constant, and this constant value agrees well with the results from the Bi and Grace model as can be seen.

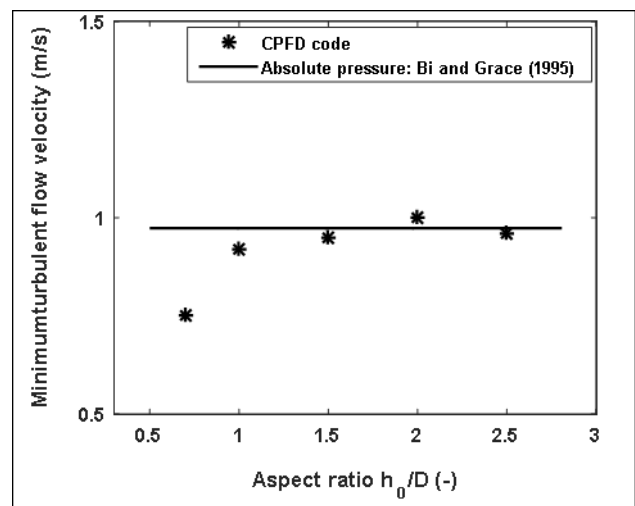


**Figure 9.** Variation of minimum turbulent flow velocity with different bed aspect ratios.

## 4 Conclusion

Fluidized bed operations are usually carried out within a given flow regime. Fluidized bed regime includes fixed bed regime, bubbling regime, slugging regime and turbulent flow regime. The static bed height may influence the transition from one regime to another, and it is therefore important to obtain how different bed

heights influences on the superficial gas velocity at the onset of each regime.

This study investigates the effect of bed height on the onset of the different fluidization regimes using the Computational Particle Fluid Dynamics (CPFD) software, Barracuda VR. The simulated results are based on sand particles with mean particle size 235  $\mu\text{m}$  and are compared with experimental data and correlations available in the literature. The simulations are carried out in a 84 mm diameter bed using height to bed diameter ratios in the range of 0.7 – 2.5. In the study, the minimum fluidization velocity is obtained at the point of maximum pressure drop from the plot of pressure drop versus the gas velocity. The superficial velocities at the onset of bubbling, slugging and turbulent flow regimes for each aspect ratio are obtained from the plot of standard deviation of the pressure drop within the bed.

The result shows that the minimum fluidization velocity drop to a stable value and the bubbling velocity remains constant with an increase in the bed height. The gas velocity at onset of slugging decreases while that of turbulent increases to a stable value as the bed height increases. Comparing with the experimental data and different correlations, the agreement in the results show that the method employed in this study for identifying different fluidized bed regimes is satisfactory.

## References

- A. R. Abrahamsen and D. Geldart (1980). Behaviour of gas-fluidized beds of fine powders part I. Homogeneous expansion. *Powder technology* **26**(1):35-46,1980. [https://doi.org/10.1016/0032-5910\(80\)85005-4](https://doi.org/10.1016/0032-5910(80)85005-4)
- C.E. Agu, C. Pfeifer, M. Eikeland, L. A. Tokheim and B.M.E. Moldestad. Models for predicting average bubble diameter and volumetric bubble flux in deep fluidized beds. *Industrial Engineering and Chemistry Research* **57**: 2658-2669, 2018. DOI: 10.1021/acs.iecr.7b04370
- J. Baeyens and D. Geldart. An investigation into slugging fluidized beds. *Chemical Engineering Science* **29**(1): 255-265, 1974. [https://doi.org/10.1016/0009-2509\(74\)85051-7](https://doi.org/10.1016/0009-2509(74)85051-7)
- W. Bauer, J. Werther and G. Emig. Influence of gas distributor design on the performance of fluidized bed reactor. *Ger. Chem. Eng* **4**: 291-298, 1981.
- H. T. Bi, N. Ellis, I. A. Abba and J. R. Grace. A state-of-the-art review of gas–solid turbulent fluidization. *Chemical Engineering Science*, **55**(21):4789-4825,2000. [https://doi.org/10.1016/S0009-2509\(00\)00107-X](https://doi.org/10.1016/S0009-2509(00)00107-X)
- Y. O. Chong, D. P. O'Dea, E. T. White, P. L. Lee and L. S. Leung. Control of the quality of fluidization in a tall bed using the variance of pressure fluctuations. *Powder Technology*, **53**(3):237-246, 1987. [https://doi.org/10.1016/0032-5910\(87\)80097-9](https://doi.org/10.1016/0032-5910(87)80097-9)
- J. S. Dennis. 3- Properties of stationary (bubbling) fluidised beds relevant to combustion and gasification systems. *Fluidized Bed Technologies for Near-Zero Emission Combustion and Gasification*, Woodhead Publishing: 77-148e,2013. <https://doi.org/10.1533/9780857098801.1.77>
- D. Escudero, and T. J. Heindel. Bed height and material density effects on fluidized bed hydrodynamics. *Chemical Engineering Science* **66**(16):3648-3655,2011. <https://doi.org/10.1016/j.ces.2011.04.036>
- C. A. S. Felipe and S. C. S. Rocha. Prediction of minimum fluidization velocity of gas–solid fluidized beds by pressure fluctuation measurements - Analysis of the standard deviation methodology. *Powder Technology* **174**(3):104-113,2007. <https://doi.org/10.1016/j.powtec.2007.01.015>
- B. C. Gourich, A. H. Vial, F. Essadki, M. Allam, B. Soulam and M. Ziyad. Identification of flow regimes and transition points in a bubble column through analysis of differential pressure signal-Influence of the coalescence behavior of the liquid phase. *Chemical Engineering and Processing: Process Intensification* **45**(3):214-223,2006. <https://doi.org/10.1016/j.ccep.2005.09.002>
- T. S. Hargest, and C. P. Artz . A New Concept in Patient Care: The Air-Fluidized Bed. *AORN journal* **10**(3): 50-53, 1969. [https://doi.org/10.1016/S0001-2092\(08\)70643-4](https://doi.org/10.1016/S0001-2092(08)70643-4)
- S. Hong, B. Jo, D. Doh and C. Choi. Determination of minimum fluidization velocity by the statistical analysis of pressure fluctuations in a gas-solid fluidized bed. *Powder Technology* **60**(3):215-221,1990. [https://doi.org/10.1016/0032-5910\(90\)80121-E](https://doi.org/10.1016/0032-5910(90)80121-E)
- D. Kunii and O. Levenspiel. *Fluidization engineering*, Elsevier, 2013
- M. Punčochář, J., Drahoš, J. Čermák and K. Selucký. EVALUATION OF MINIMUM FLUIDIZING VELOCITY IN GAS FLUIDIZED BED FROM PRESSURE FLUCTUATIONS. *Chemical Engineering Communications*. **35**(1-6):81-87,1985. <https://doi.org/10.1080/00986448508911219>
- R. Sarker, M. Rahman, N. Love and A. Choudhuri (2012). Effect of Bed Height, Bed Diameter and Particle Shape on Minimum Fluidization in a Gas-Solid Fluidized Bed. *50th AIAA Aerospace Sciences Meeting including the New Horizons Forum and Aerospace Exposition*. DOI: 10.2514/6.2012-644
- W. M. Tchowa, A. R. Alvaro and A. Schumpe. Flow regime transitions in a bubble column. *Chemical Engineering Science* **170**:263-269, 2017. <https://doi.org/10.1016/j.ces.2017.04.010>
- C. Vial, E. Camarasa, S. Poncin, G. Wild, N. Midoux and J. Bouillard. Study of hydrodynamic behaviour in bubble columns and external loop airlift reactors through analysis of pressure fluctuations. *Chemical Engineering Science* **55**(15): 2957-2973, 2000. [https://doi.org/10.1016/S0009-2509\(99\)00551-5](https://doi.org/10.1016/S0009-2509(99)00551-5)
- J. Yates, (2013). *Fundamentals of Fluidized-Bed Chemical Processes: Butterworths Monographs in Chemical Engineering*, Butterworth-Heinemann.
- J. Yerushalmi, and N. T. Cankurt (1979). Further studies of the regimes of fluidization. *Powder Technology* **24**(2): 187-205. [https://doi.org/10.1016/0032-5910\(79\)87036-9](https://doi.org/10.1016/0032-5910(79)87036-9)